

***Ab initio* characterization of low-lying triplet state potential-energy surfaces and vibrational frequencies in the Wulf band of ozone**

Daiqian Xie^{a)} and Hua Guo^{b)}

Department of Chemistry, University of New Mexico, Albuquerque, New Mexico 87131

Kirk A. Peterson

Department of Chemistry, Washington State University, Richland, Washington 99352 and the Environmental Molecular Sciences Laboratory, Pacific Northwest National Laboratory, Richland, Washington 99352

(Received 16 August 2001; accepted 21 September 2001)

Accurate *ab initio* potential-energy surfaces of the 3A_2 and 3B_1 states of ozone and their nonadiabatic coupling are reported near the ground-state equilibrium geometry using an internally contracted multireference configuration interaction method. These coupled three-dimensional potential-energy surfaces enable the first theoretical characterization of all three vibrational modes in the Wulf band. Reasonably good agreement with recent experimental observations is obtained.

© 2001 American Institute of Physics. [DOI: 10.1063/1.1417502]

I. INTRODUCTION

The photochemistry of the ozone (O_3) molecule plays a central role in many important processes in the earth's upper atmosphere.¹ Its absorption starts in near infrared (Wulf band) and extends to visible (Chappius band) and ultraviolet (Huggins and Hartley bands) regions.² These absorption bands all have diffuse structures, indicative of strong predissociation. It is thus difficult to spectroscopically extract information about the structure and rovibrational dynamics. Consequently, theoretical investigations are indispensable in helping to interpret the spectra and understanding the dynamics. In fact, it is the interplay between theory and experiment that has greatly advanced our understanding of this complex system. This is particularly true for the weak Wulf band from 10 000 to 15 000 cm^{-1} .³

Experimental study of the Wulf band has been difficult because of its extremely low intensity. As a result, the electronic character of the excited state has been misassigned as a singlet until recently.⁴ The correct assignment to triplet (3A_2 with possible contribution from 3B_1) states was first made theoretically based on high level *ab initio* calculations.⁵⁻⁷ The singlet-triplet transition, facilitated by spin-orbit coupling with higher singlet states, explains the low intensity of the absorption. Theory was even able to assign the vibrational progression in this band. Both the electronic and vibrational assignments were later placed on firm experimental footing by high-resolution spectroscopic analysis of the rotational structure of several low-lying vibrational features.⁸⁻¹⁴

It is now well established that there are three low-lying triplet (3B_2 , 3A_2 , and 3B_1) states that are involved in the Wulf band absorption.^{5-7,15-17} Absorption to the 3B_2 state can be neglected because of extremely small oscillator strength.^{6,7} The vibrational features in the Wulf band can be

predominately attributed to the 3A_2 state, which mixes with the higher 3B_1 state. All three triplet states are energetically higher than the ground-state dissociation limit,¹⁶⁻²⁰ although significant dissociation barriers exist.

The triplet states involved in the Wulf band may impact several kinetic, isotopic, and spectroscopic issues related to ozone chemistry.⁹ For instance, the recombination reaction between $O(^3P)$ and $O_2(^3\Sigma^-)$ may be influenced by the participation of the 3A_2 and/or 3B_2 states which correlate to the same asymptotic limit of the ground electronic state. If long-lived metastable states exist on these PESs, they may also provide an efficient reservoir for the "missing" ozone in the upper atmosphere. These and other related effects are important for developing accurate atmospheric models.

Despite the wealth of experimental and theoretical knowledge gained in the past decades, there are still quite a few unresolved issues related to the Wulf band. For example, the antisymmetric vibrational frequency of the 3A_2 state is quite uncertain. Experimentally, the symmetric stretching and bending frequencies ($\nu_1 = 1190 \pm 15$ cm^{-1} and $\nu_2 = 529.4 \pm 0.7$ cm^{-1}) have been determined from the vibrational features in the Wulf band,^{4,9,14} but the antisymmetric stretching frequency was estimated from the triplet state zero-point energy ($\nu_3 = 367 \pm 17$ cm^{-1}).¹⁴ Theoretical results to date provide little insight since most *ab initio* calculations have been either restricted to the C_{2v} geometry^{5-7,16} or limited in a few cuts of the PESs.¹⁵ Other outstanding questions include the mechanism and dynamics of the observed predissociation of nearly all the rovibrational levels.¹¹⁻¹³ Apparently, such questions cannot be answered definitively without a clear picture of the three-dimensional topology of the relevant PESs and the nonadiabatic interaction between the 3A_2 and 3B_1 states.

II. COMPUTATIONAL DETAILS

In this work, we report the first three-dimensional high level *ab initio* calculation of the near-equilibrium PESs of the 3A_2 , and 3B_1 states of ozone and their nonadiabatic in-

^{a)}Visiting Professor from Department of Chemistry, Sichuan University, Chengdu, Sichuan, P. R. China.

^{b)}Corresponding author. Electronic mail: hguo@unm.edu

teraction. Like our previous work on the ground-state ozone,²¹ the calculation was carried out using the MOLPRO suite of *ab initio* programs.²² The 3B_2 state, which as been shown to possess a negligible oscillator strength,^{6,7} was not considered. We also ignored the spin-orbit coupling and concentrated on the three-dimensional topology of the PESs, as well as the corresponding vibrational frequencies.

The results reported here were obtained with Dunning's correlation consistent triple-zeta (cc-pVTZ) basis set for the oxygen atoms.²³ The basis set was augmented by a set of diffuse functions ($1s, 1p$) taken from the standard aug-cc-pVTZ basis set.²⁴ A total of 102 contracted functions were employed. This basis is smaller than that used in our ground-state calculation,²¹ mainly because of computational restraints, but larger than the recent PES calculation of the singlet states.²⁵ The internally contracted multireference configuration interaction (icMRCI) was based on the state-averaged complete active space self-consistent field (CASSCF) orbitals. The active space consists of the 9 orbitals arising from the $2p$ atomic orbitals of oxygen for the 12 valence electrons. The $1s$ and $2s$ inner orbitals were fully optimized, but constrained to be doubly occupied. This led to a total of 1710 configuration state functions (CSFs) in C_s symmetry. In the subsequent MRCI calculations, the reference function was the same as the CASSCF active space and the six low-lying orbitals were frozen. All single and double excitations with respect to the reference function were included and the doubly external configurations were internally contracted.²⁶ The total number of configurations was about 0.7 million, while the number of uncontracted configurations was about 44 million. In order to take into account higher excitations, the Davidson correction was employed.²⁷

The 3A_2 and 3B_1 states cross at C_{2v} geometry, but interact at C_s as A'' states. As discussed earlier, the nonadiabatic interaction between the two states is essential in understanding the spectrum and dynamics. To this end, we have calculated the quasidiabatic energies of these two states and their interaction, using the method of Werner and co-workers.²⁸ The quasidiabatization transforms both the orbitals and CI vectors to minimize their changes from the C_{2v} reference. A distinct advantage of the method is the expression of the PESs as a 2×2 potential matrix, which is immediately amenable to quantum studies. In addition, the PESs in the diabatic representation are generally much smoother and better behaved than their adiabatic counterparts. A similar method has been used to generate the singlet PESs for the Chappius band of ozone.²⁵

III. RESULTS

The adiabatic and diabatic potential energies as well as the nonadiabatic coupling were computed on a three-dimensional grid in the internal coordinates (R_1, R_2, θ), where R_1 and R_2 are the two bond lengths and θ is the enclosed bond angle. One of the distances was varied in the range $[2.1, 4.0] a_0$, the other one within $[2.1, 3.1] a_0$, and the angle was varied between 75 and 155° . The calculations are computational intensive, with each point costing approximately 1.5–2.0 hour on a 500 Mhz Compaq Alpha (EV6)

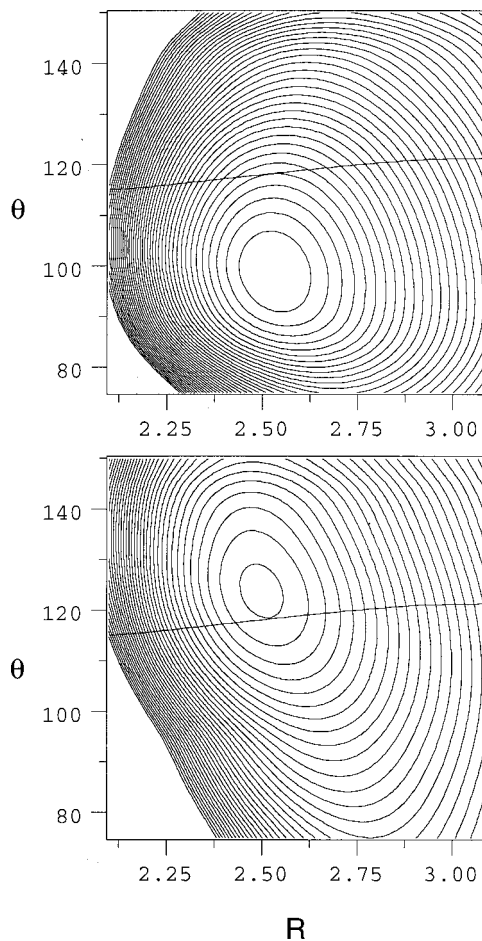


FIG. 1. Diabatic potentials of the 3A_2 (upper panel) and 3B_1 (lower panel) states at C_{2v} . The crossing seam is also displayed in the plots. The contour interval is 0.1 eV.

workstation. A total of 739 symmetry unique points were selected. The final PESs were interpolated using a three-dimensional cubic spline method.

Both the 3A_2 and 3B_1 PESs have their minima in C_{2v} as shown by Fig. 1. The equilibrium geometries are listed in Table I. Between the two, the equilibrium of the 3A_2 state is much better determined. Our results are in good agreement with the latest experimental values derived from rotational constants.¹² For the 3B_1 state, no equilibrium geometry has been measured, but our results are consistent with previous *ab initio* data. The calculated adiabatic excitation energy (T_e) and band origin (T_0) of the 3A_2 state also agree well with experimental values obtained from different sources.^{12,14,18} The T_e value of the 3B_1 state is somewhat larger than the reported experimental value.^{9,18} However, the latter may contain significant uncertainty. Our results reaffirm that both triplet states are above the dissociation limit of the ground electronic state ($D_0 = 1.13$ eV). The excess energy of the well-characterized 3A_2 state is 0.13 eV, in good agreement with experimental estimate of ~ 0.1 eV.

As shown in Fig. 1, the 3A_2 and 3B_1 PESs cross near their minima. The crossing seam is nearly independent of the O–O bond lengths and located approximately at 115° . The corresponding adiabatic PESs form a conical intersection

TABLE I. Calculated and observed equilibrium geometries and excitation energies.^a

State	Method	R_e	θ_e	T_e	T_0	T_v
3A_2	MRD-CI ^b	1.36	100	0.90	0.86 ^c	1.73
	CASPT2 ^d	1.344	97.8	1.16	1.12 ^c	1.77
	MRMP ^c	1.369	99.2	0.90	0.88 ^c	1.65
	MRCI+Q (Diabatic)	1.332	99.1	1.30	1.26 ^c	1.94
	Expt.	1.345 ^f	98.9 ^f	1.235 ^g	1.18 ^{f,g,h}	
3B_1	MRD-CI ^b	1.35	~ 122.5	1.49	...	1.91
	CASPT2 ^d	1.310	129.8	1.35	...	1.62
	MRMP ^c	1.348	123.7	1.18	...	1.51
	MRCI+Q (Diabatic)	1.315	123.8	1.77	...	1.98
	Expt.			1.48 ⁱ	1.45 ^{h,i}	

^aThe bond length is in angstrom, the angle in degree and the energy in eV.

^bReference 15.

^cValues derived using the zero-point energy calculated in this work.

^dReference 17.

^eReference 16.

^fReference 12.

^gReference 14.

^hReference 18.

ⁱReference 9.

near the C_{2v} seam. The lower adiabat retains the minimum of the 3A_2 state, while the upper adiabat forms a minimum near the crossing seam. In Fig. 2, the adiabatic, diabatic, and nonadiabatic PESs are plotted in the two O–O stretching coordinates at $\theta=99^\circ$. Both the diabatic PESs are quasibound and they strongly interact with each other via the nonadiabatic coupling, which varies smoothly with the coordinates and is antisymmetric with respect to the exchange of the two O–O bonds. The resultant upper adiabat is strongly quasibound and correlated to the $O(^3P)+O_2(^1\Delta_g)$ asymptote. The lower adiabat, which is most relevant to the Wulf band,

has a shallow minimum, which is separated from the $O(^3P)+O_2(^3\Sigma^-)$ dissociation limit by a barrier, which is located at $R_1=2.98 a_0$, $R_2=2.33 a_0$, and $\theta=104.6^\circ$, with a height of 0.095 eV.

Since both PESs are quasibound relative to the $O(^3P)+O_2(^3\Sigma^-)$ asymptote, the vibrational levels are predissociative. We have determined both energy positions and lifetimes of several low-lying vibrational levels using a complex-symmetric Lanczos algorithm.^{29,30} The calculation was carried out on a discretized Radau (r_1, r_2, χ) coordinate grid of the size $n_{r_1} \times n_{r_2} \times n_\chi = 60 \times 60 \times 50$. A negative

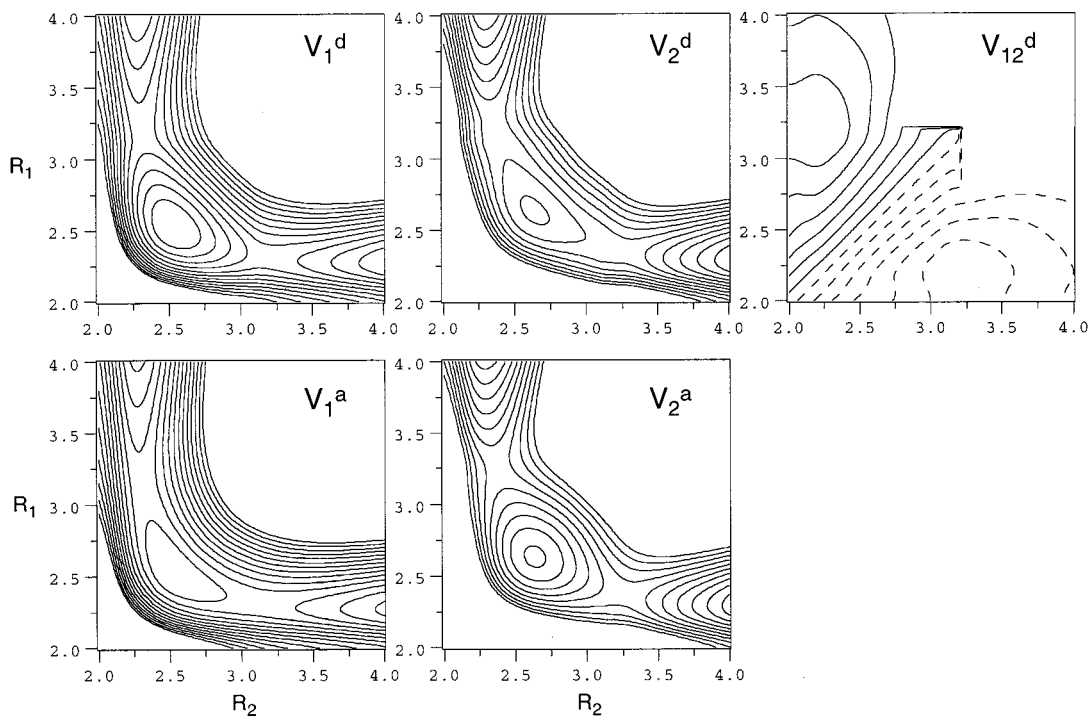


FIG. 2. Diabatic and adiabatic potentials of the two $^3A''$ states at $\theta=99^\circ$. The contour interval is 0.1 eV and dashed lines indicate negative contours. The artificial features in V_{12}^d at large R_1, R_2 are due to the truncation of the grid.

TABLE II. Positions and widths (in cm^{-1}) of low-lying resonance states.^a

Level	Re(E)	Γ	E_{exp}^b
(000)	0.0(0.0)	0.0009(0.0009)	
(001)	422.2(427.3)	4.02(3.52)	367 \pm 17
(010)	496.6(501.5)	9.54(9.04)	529.4 \pm 0.7
(020)	1002.5(1010.3)	98.4(98.1)	
(100)	1180.4(1179.4)	44.1(49.3)	1190 \pm 15
ZPE	1103.6		1046

^aValues in parentheses were calculated using the adiabatic potentials.

^bReference 14.

imaginary potential was placed at the edges of the radial grids. The strength of the absorption potential was varied in search of the stabilization point of each resonance. The calculation was performed in the diabatic representation with the nonadiabatic coupling.

Table II lists resonance energies Re(E) and widths Γ ($=2\text{Im}(E)$) for several lowest-lying vibrational levels up to 1200 cm^{-1} above the zero-point energy. Three quantum numbers for the symmetric stretching, bending, and antisymmetric stretching modes were assigned to each level. Higher-energy levels are not reported because of limitations of the PESs. Our calculations yielded the fundamental frequencies for all three vibrational modes. Both the symmetric stretching and bending frequencies are in reasonable agreement with experimental values. For the antisymmetric stretching mode, our result of 422.2 cm^{-1} is consistent with the experimentally estimated value of 367 cm^{-1} .¹⁴ We stress that estimation from the zero-point energy can be misleading since the excited states are very anharmonic, particularly in the antisymmetric stretching coordinate. Our calculated zero-point energy (1103.5 cm^{-1}) is also close to the observed value (1046 cm^{-1}).¹⁴ Much of the remaining error can be attributed to not correlating the oxygen $2s$ -like electrons in the MRCI treatment. Calculations have also been carried out on adiabatic PESs without the nonadiabatic coupling and the results are listed in parentheses in Table II. The small difference with those obtained with coupled diabatic potentials indicates that the system is close to the adiabatic limit.

All vibrational levels were found to predissociate. The ground vibrational level is the most stable, with a lifetime ($\tau=1/\Gamma$) of approximately 5.9 ns. This is consistent with experimental observations of rotational contours.^{8,9} The relatively long lifetime can be attributed to the fact that this is the only vibrational state below the adiabatic dissociation barrier. Higher overtones are significantly more predissociative as they are all above the barrier. The (011) and (002) levels are so short-lived that their energies and lifetimes cannot be accurately determined. As a result, they are not listed in the table. The lifetimes of other levels in the energy region are in the picosecond and subpicosecond range, in good agreement with experimental estimates of the predissociation lifetime, which range from 0.1 ps¹¹ to 1 ns.¹³ We do caution, however, that our calculation ignored the potentially more efficient predissociation channel via the ground-electronic state.

IV. SUMMARY

To summarize, we have calculated the near-equilibrium PESs of two low-lying triplet states of ozone and determined the frequencies of all three vibrational modes. Our investigation clarified a number of important issues regarding the Wulf band of ozone. In particular, we reconfirmed that both the 3A_2 and 3B_1 states are quasibound with C_{2v} minima above the ground-state dissociation limit. The three-dimensional PESs allowed us to study low-lying predissociative vibrational states. To this end, we reported both positions and widths of several such resonance states. The vibrational frequencies are in good agreement with known experimental values. We stress that the PESs reported here are certainly not of spectroscopic accuracy, but they should provide a reasonably reliable picture of the nuclear dynamics. We are in the process of generating more *ab initio* points for studying the nonadiabatic dissociation dynamics.

ACKNOWLEDGMENTS

The authors acknowledge financial support by the U.S. National Science Foundation (HG, CHE-0090945), the National Natural Science Foundation of China (DX, Grant Nos. 29872162 and 29973072), and the Chemical Sciences Division in the Office of Basic Energy Sciences of the U.S. Department of Energy (KAP). The William R. Wiley Environmental Molecular Sciences Laboratory (EMSL) is located at the Pacific Northwest National Laboratory (PNNL). Operation of the EMSL is funded by the Office of Biological and Environmental Research in the U.S. Department of Energy (D.O.E). The Pacific Northwest National Laboratory is operated by Battelle for the U.S. Department of Energy under Contract No. DE-AC06-76RLO 1830.

- J. I. Steinfeld, S. M. Alder-Golden, and J. W. Gallagher, *J. Phys. Chem. Ref. Data* **16**, 911 (1987).
- R. Bacis, A. J. Bouvier, and J. M. Flaud, *Spectrochim. Acta, Part A* **54**, 17 (1998).
- O. R. Wulf, *Proc. Natl. Acad. Sci. (Paris)* **16**, 507 (1930).
- S. M. Anderson, J. Morton, and K. Mauersberger, *J. Chem. Phys.* **93**, 3826 (1990).
- M. Braunstein and R. T. Pack, *J. Chem. Phys.* **96**, 6378 (1992).
- M. Braunstein, R. L. Martin, and P. J. Hay, *J. Chem. Phys.* **102**, 3662 (1995).
- B. Minaev and H. Ågren, *Chem. Phys. Lett.* **217**, 531 (1994).
- S. M. Anderson, P. Hupalo, and K. Mauersberger, *J. Chem. Phys.* **99**, 737 (1993).
- S. M. Anderson and K. Mauersberger, *J. Geophys. Res.* **100**, 3033 (1995).
- A. J. Bouvier, R. Bacis, B. Bussery *et al.*, *Chem. Phys. Lett.* **255**, 263 (1996).
- B. Abel, A. Charvat, and S. F. Deppe, *Chem. Phys. Lett.* **277**, 347 (1997).
- A. J. Bouvier, D. Inard, V. Veyret *et al.*, *J. Mol. Spectrosc.* **190**, 189 (1998).
- D. Inard, A. J. Bouvier, R. Bacis, S. Churassy, F. Bohr, J. Brion, J. Malicet, and M. Jacon, *Chem. Phys. Lett.* **287**, 515 (1998).
- J. Günther, S. M. Anderson, G. Hilpert, and K. Mauersberger, *J. Chem. Phys.* **108**, 5449 (1998).
- A. Banichivich, S. D. Peyerimhoff, and F. Grein, *Chem. Phys.* **178**, 155 (1993).
- T. Tsuneda, H. Nakano, and K. Hirao, *J. Chem. Phys.* **103**, 6520 (1995).
- P. Borowski, M. Fülischer, P.-A. Malmqvist, and B. O. Roos, *Chem. Phys. Lett.* **237**, 195 (1995).
- D. W. Arnold, C. Xu, E. H. Kim, and D. M. Neumark, *J. Chem. Phys.* **101**, 912 (1994).
- M. Allan, N. J. Mason, and J. H. Davies, *J. Chem. Phys.* **105**, 5665 (1996).

- ²⁰M. C. Garner, K. A. Hanold, M. S. Resat, and R. E. Continetti, *J. Phys. Chem.* **101**, 6577 (1997).
- ²¹D. Xie, H. Guo, and K. A. Peterson, *J. Chem. Phys.* **112**, 8378 (2000).
- ²²MOLPRO is a package of *ab initio* programs written by H.-J. Werner and P. J. Knowles with contributions from R. D. Amos, D. L. Cooper, M. J. O. Deegan *et al.*
- ²³T. H. Dunning, *J. Chem. Phys.* **90**, 1007 (1989).
- ²⁴R. A. Kendall, T. H. Dunning, and R. J. Harrison, *J. Chem. Phys.* **96**, 6796 (1992).
- ²⁵C. Woywod, M. Stengle, W. Domcke, H. Flöthmann, and R. Schinke, *J. Chem. Phys.* **107**, 7282 (1997).
- ²⁶H.-J. Werner and P. J. Knowles, *J. Chem. Phys.* **89**, 5803 (1988).
- ²⁷S. R. Langhoff and E. R. Davidson, *Int. J. Quantum Chem.* **8**, 61 (1974).
- ²⁸D. Simah, B. Hartke, and H.-J. Werner, *J. Chem. Phys.* **111**, 4523 (1999).
- ²⁹J. K. Cullum and R. A. Willoughby, *Lanczos Algorithms for Large Symmetric Eigenvalue Computations* (Birkhauser, Boston, 1985).
- ³⁰D. Xie, R. Chen, and H. Guo, *J. Chem. Phys.* **112**, 5263 (2000).